Наномеханика

Nanomechanics of materials and systems

Lecture 13

MEMS and NEMS sensors

МЭМС и НЭМС датчики

Дизайн МЭМС и НЭМС Design of MEMS&NEMS

- Принцип работы
- Набор элементов системы
  - пассивные
  - датчики
  - актуаторы (приводы)
- Анализ, расчет, моделирование
  - предельно достижимые параметры
  - погрешности и шумы
  - предельные эксплуатационные параметры
- Разработка технологии
  - последовательность этапов технологии
  - оборудование и материалы
  - себестоимость производства
- Разработка отдельных этапов
  - определение режимов технологических процессов
  - совместимость различных этапов

- Operation principles
- Set of system elements
  - passive
  - sensors
  - actuators
- Analysis, calculation, modeling
  - Achievable parameters
  - Precision and noise
  - Operation parameters and limitations
- Development of technology
  - Sequence of technological stages
  - Equipment and materials
  - Production cost
- Development of individual stages
  - conditions of technological processes
  - Consistency of different technological stages

Датчики в различных устройствах МЭМС/НЭМС
MEMS&NEMS sensor applications

- Транспорт Transportation
  - Автомобильная безопасность, системы торможения и остановки Safety and braking systems
  - Управление двигателями и силовыми установками Engine control
  - Распределенные датчики контроля Distributed monitoring
  - Системы навигации Navigation systems
- Биология и медицина Biology and medicine
  - Миниатюрные биохимические аналитические инструменты Analytical instruments
  - Кардиологические управляющие системы Cardiologic control systems
  - Системы доставки лекарств (инсулин, анальгетики) Drug delivery (insulin, analgesics)
  - Нейростимуляторы Neurostimulators
- Компоненты оптических систем, в том числе волоконно-оптической связи Components of optical systems, including communications
- Радио и беспроводная электроника Radio and wireless electronics
- Военные и специальные системы Military and special systems

Термоэлектрический датчик
Thermoelectric sensor

$$\Delta V = (\alpha_2 - \alpha_1)(T_{hot} - T_{cold})$$

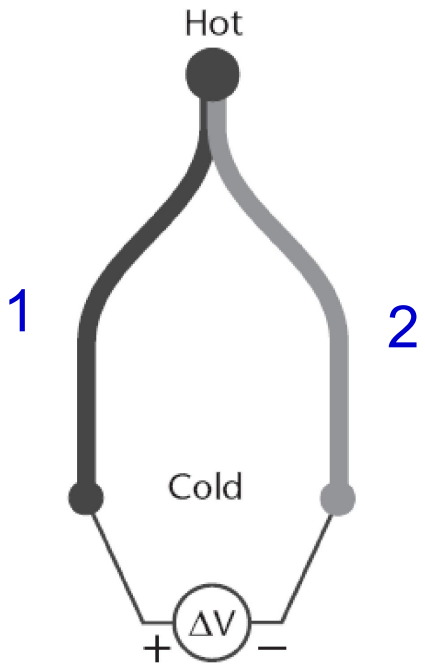

Коэффициенты Зеебека по отношению к платине для некоторых металлов и поликремния. Seebeck coefficients.

	μV/K		μV/K
Bi	–73.4	Ag	7.4
Ni	–14.8	Cu	7.6
Pa	–5.7	Zn	7.6
Pt	0	Au	7.8
Ta	3.3	W	11.2
Al	4.2	Mo	14.5
Sn	4.2	*n*-poly (30 Ω/□)	–100
Mg	4.4	*n*-poly (2600 Ω/□)	–450
Ir	6.5	*p*-poly (400 Ω/□)	270

Note: The sheet resistance is given for the 0.38-μm-thick polysilicon films.

Датчик на основе *pn*-перехода
P-N junction temperature sensor

Вольт-амперная характеристика полупроводникового диода

$$J = J_s(e^{eV/nkT} - 1)$$

$$J_s \sim T^{3+\gamma/2} \exp(-E_g / kT)$$

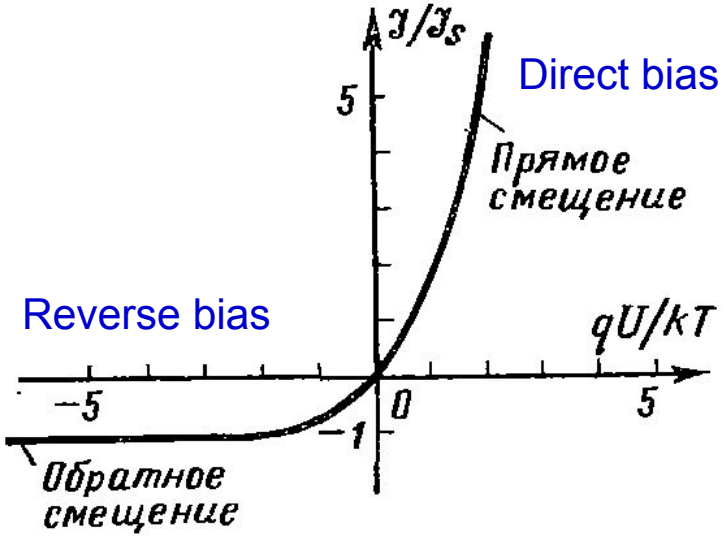

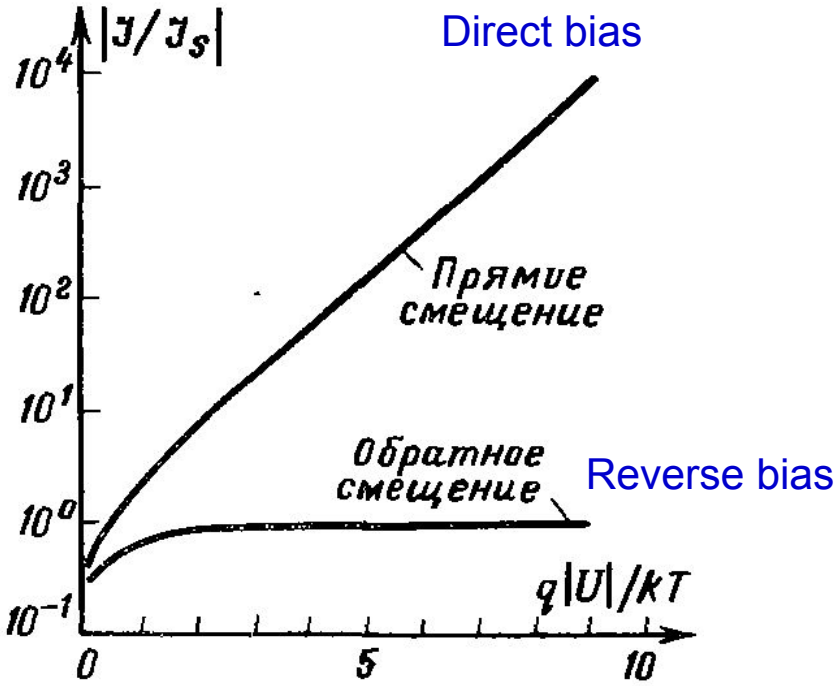

Терморезистивный датчик Thermistor

- Большой терморезистивный коэффициент (0.2-0.3 %/K)
  Large temperature coefficient of resistance
- Малая теплоемкость
  Small thermal capacitance
- Низкий шум
  (limit is thermal and *1/f* noise)
  Low thermal noise
- Малая инерционность
  Small thermal inertia
- Малая теплопроводность
  (the theoretical lowest limit is 10^{-9} W/K due to radiative heat loss)
  Small thermal conductivity

$$c = \frac{Q}{m\Delta T}$$

Физические свойства некоторых материалов НЭМС
Physical properties of some NEMS materials

Property[a]	*Si*	SiO_2	Si_3N_4	*Quartz*	*SiC*	*Diamond*	*GaAs*	*AlN*	92% Al_2O_3	*Polyimide*	*PMMA*
Relative permittivity (ε_r)	11.7	3.9	4–8	3.75	9.7	5.7	13.1	8.5	9	—	—
Dielectric strength (V/cm $\times 10^6$)	0.3	5–10	5–10	25–40	4	10	0.35	13	11.6	1.5–3	0.17
Electron mobility ($cm^2/V{\cdot}s$)	1,500	—	—	—	1,000	2,200	8,800	—	—	—	—
Hole mobility ($cm^2/V{\cdot}s$)	400	—	—	—	40	1,600	400	—	—	—	—
Bandgap (eV)	1.12	8-9	—	—	2.3–3.2	5.5	1.42	—	—	—	—
Young's modulus (GPa)	160	73	323	107	450	1,035	75	340	275	2.5	3
Yield/fracture strength (GPa)	7	8.4	14	9	21	>1.2	3	16	15.4	0.23	0.06
Poisson's ratio	0.22	0.17	0.25	0.16	0.14	0.10		0.31	0.31	0.34	—
Density (g/cm^3)	2.4	2.2	3.1	2.65	3.2	3.5	5.3	3.26	3.62	1.42	1.3
Coefficient of thermal expansion ($10^{-6}/°C$)	2.6	0.55	2.8	0.55	4.2	1.0	5.9	4.0	6.57	20	70
Thermal conductivity at 300K ($W/m{\cdot}K$)	157	1.4	19	1.4	500	990–2,000	0.46	160	36	0.12	0.2
Specific heat ($J/g{\cdot}K$)	0.7	1.0	0.7	0.787	0.8	0.6	0.35	0.71	0.8	1.09	1.5
Melting temperature (°C)	1,415	1,700	1,800	1,610	1,800[b]	3,652[b]	1,237	2,470	1,800	380[c]	90[c]

Инфракрасные датчики и массивы датчиков
Infrared sensors and their arrays

Материалы: $La_{1-x}A_xMnO_3$; A = Ca, Sr, Ba, or Pb, VO_2, V_2O_3, and V_2O_5

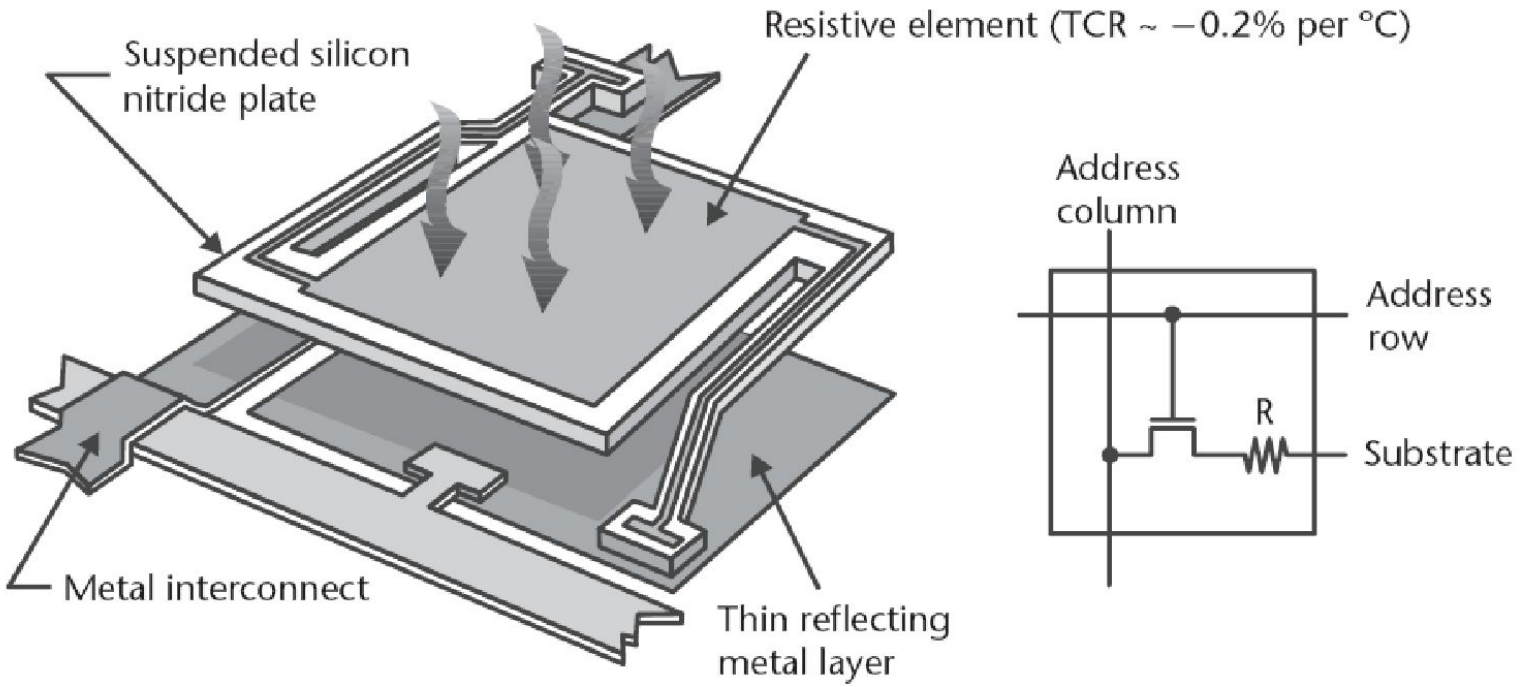

Illustration of a single sense element in the infrared imaging array from Honeywell. Incoming infrared radiation heats a sensitive resistive element suspended on a thin silicon nitride plate. Electronic circuits measure the change in resistance and infer the radiation intensity. Typical array is 240 x 336 pixels. The estimated change in temperature for an incident radiation power of 10^{-8} W is only 0.1ºC. The corresponding resistance change is a measurable –10Ω for a 50-kΩ resistor. The thermal capacity of a pixel is 10^{-9} J/K. The thermal response time is less than 10 ms.

Датчик газового потока Gas flow sensor

Gas flow rates are in the range of 0 to 1,000 sccm. The full-scale output is approximately 75 mV, and the response time is less than 3 ms. The device consumes less than 30 mW.

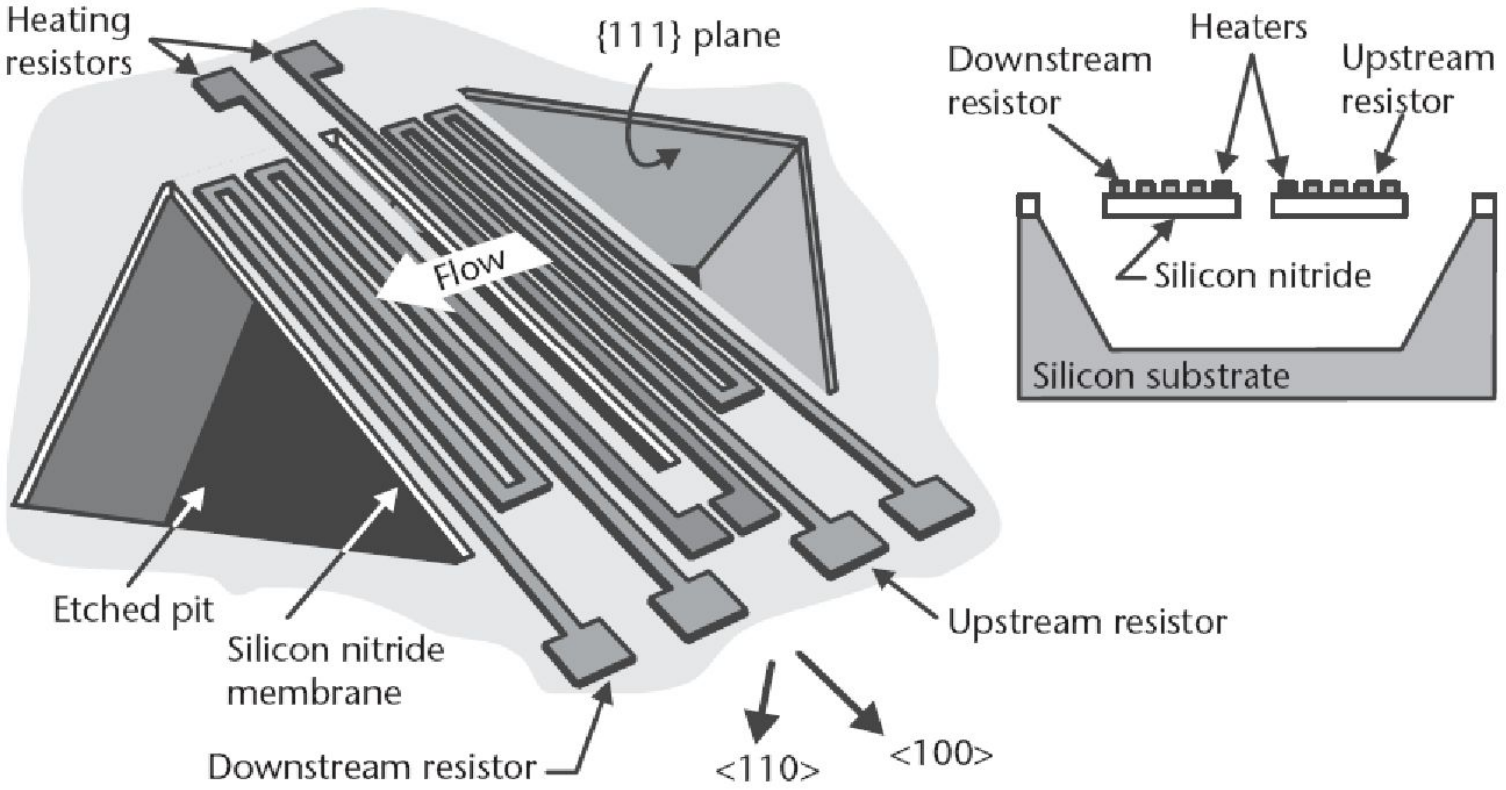

Illustration of a micromachined mass flow sensor. Gas flow cools the upstream heater and heats the downstream heater. Temperature-sensitive resistors are used to measure the temperature of each heater and consequently infer the flow rate. The etched pit underneath the heater provides exceptional thermal isolation to the silicon support frame. (*After:* technical sheets on the AWM series of mass airflow sensors, Honeywell, Inc., Minneapolis, Minnesota, USA.)

Датчик CO - Carbon monoxide sensor

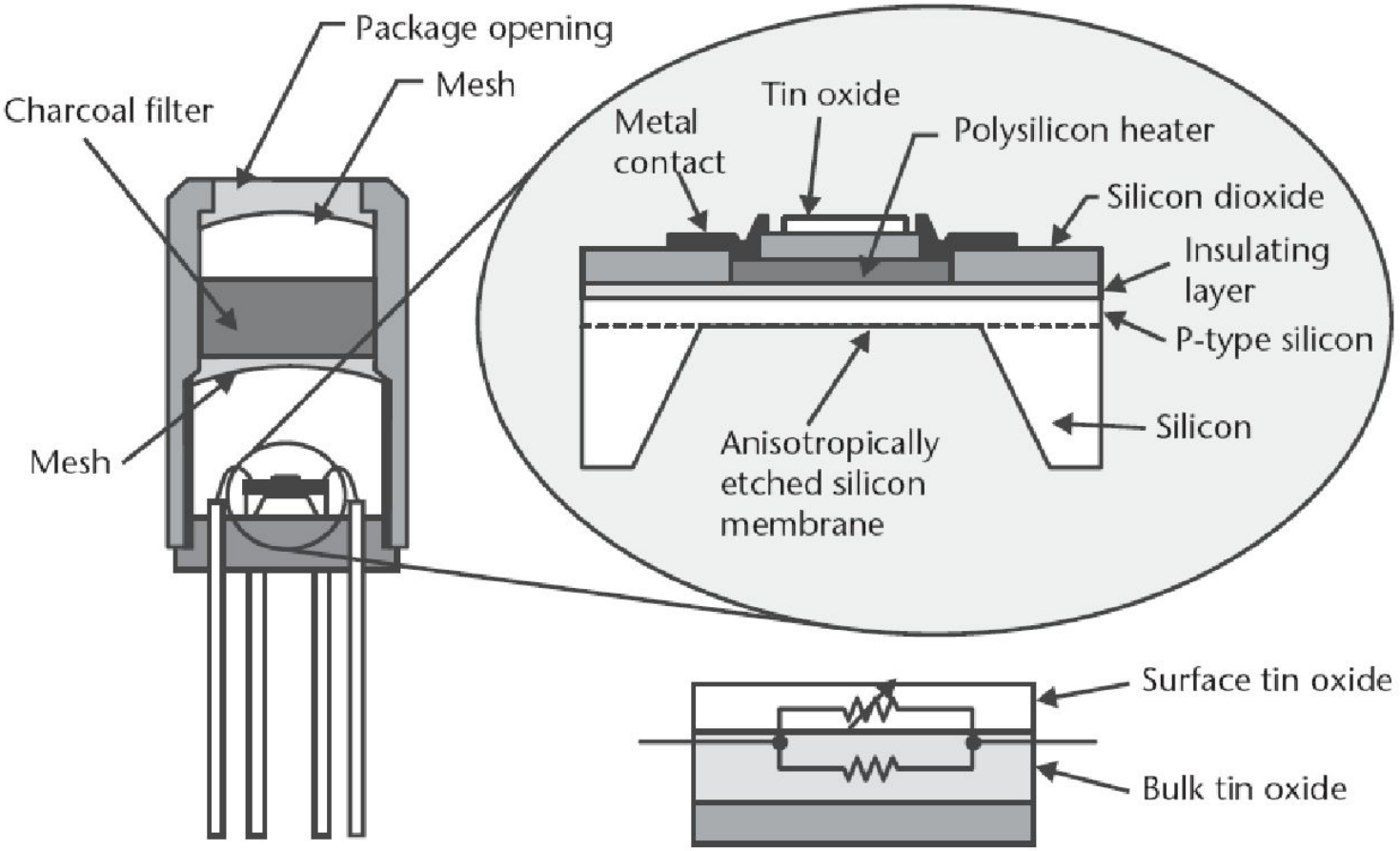

Illustration of a carbon monoxide sensor, its equivalent circuit model, and the final packaged part. The surface resistance of tin-oxide changes in response to carbon monoxide. A polysilicon heater maintains the sensor at a temperature between 100° and 450ºC in order to reduce the adverse effects of humidity.

Пьезорезистивный датчик Piezoresistors

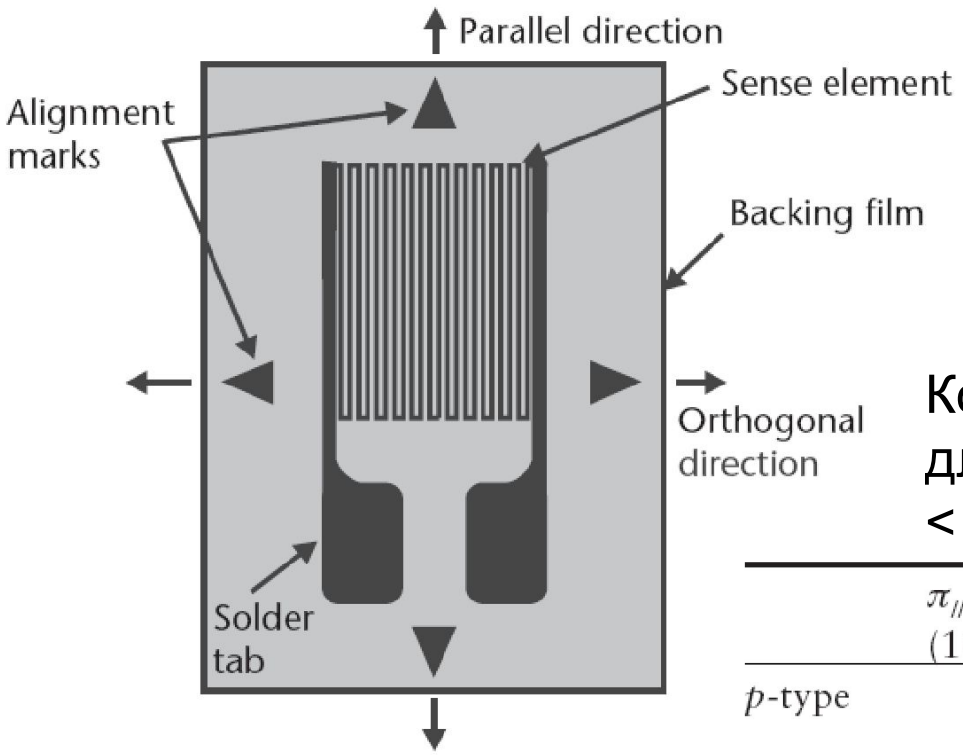

Активный элемент – Si или поли-Si

Пьезосопротивление:

$$\Delta\rho/\rho = \pi_{//}\sigma_{//} + \pi_{\perp}\sigma_{\perp}$$

Коэффициенты пьезосопротивления для Si при концентрации носителей < 10^{18} cm^{-3}. Piezoresistance of Si

	$\pi_{//}$ (10^{-11} m^2/N)	$\pi_{\perp}$ (10^{-11} m^2/N)	
p-type	7	–1	In <100> direction
	72	–66	In <110> direction
n-type	–102	53	In <100> direction
	–31	–18	In <110> direction

A typical thin metal foil strain gauge mounted on a backing film. Stretching of the sense element causes a change in its resistance.

Пьезорезистивный датчик давления
Piezoresistive pressure sensor

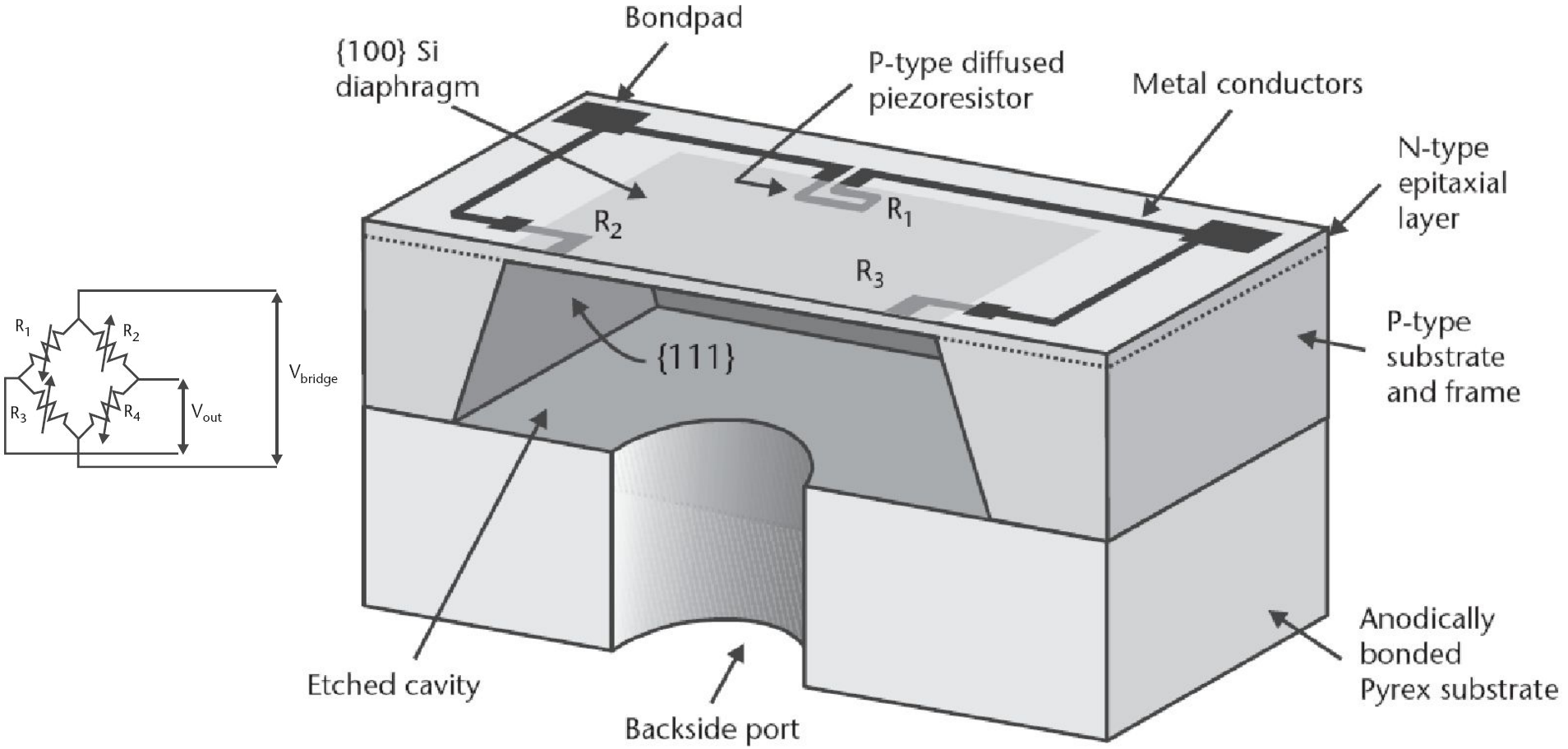

The calibration and compensation functions are provided by specially designed application-specific integrated circuits (ASICs). The active circuits amplify the voltage output of the piezoresistive bridge to standard CMOS voltage levels (0–5V). They also correct for temperature errors and nonlinearities. Error coefficients particular to individual sensors are permanently stored in on-board electrically programmable memory.

Последовательность производства датчика давления
Technological stages of pressure sensor

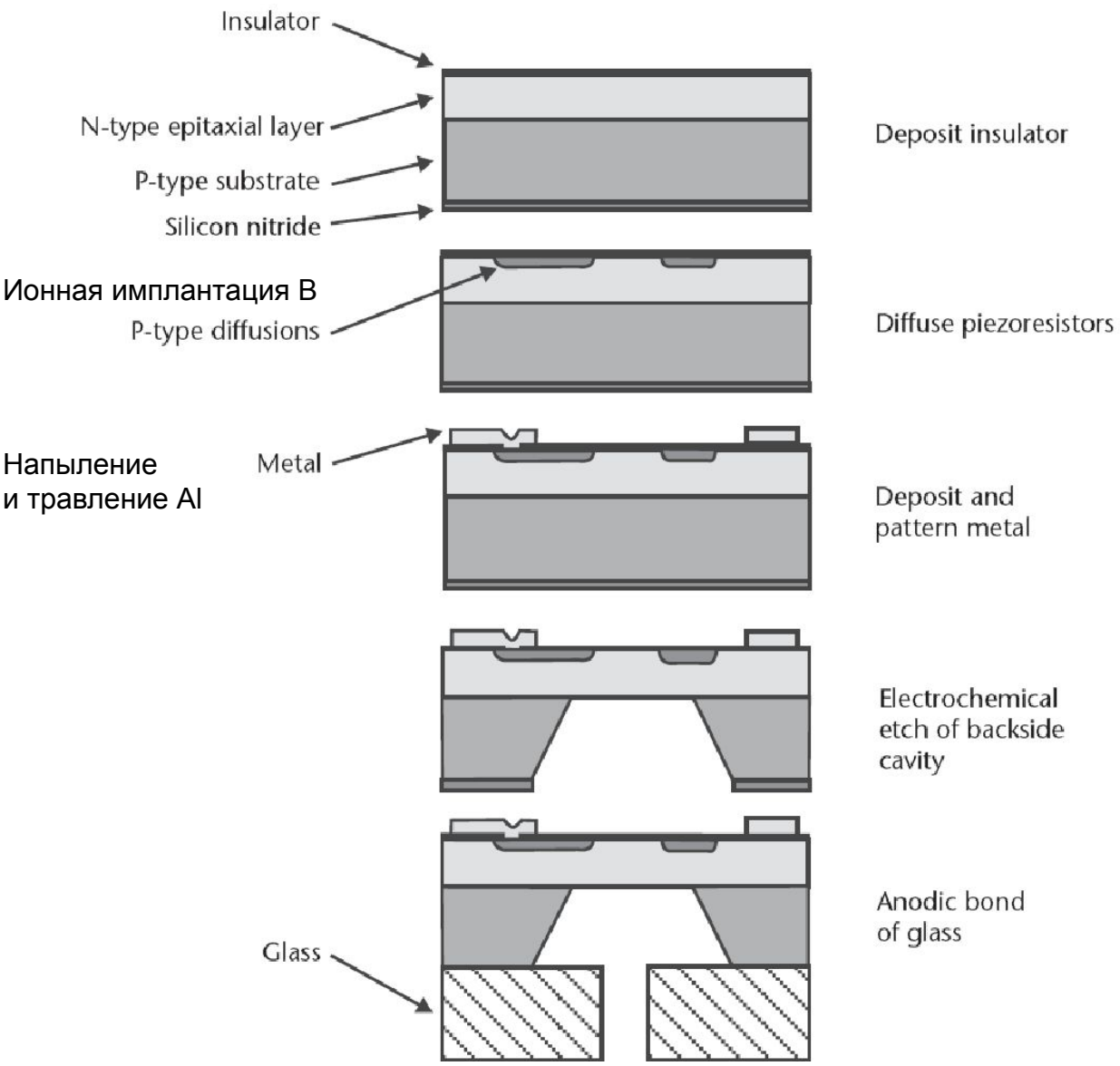

The first high-volume production of a pressure sensor began in 1974 at National Semiconductor Corp. of Santa Clara, California. Pressure sensing has since grown to a large market with an estimated 60 million silicon micromachined pressure sensors manufactured in 2001.

Миниатюрный абсолютный пьезорезистивный датчик давления. Absolute pressure sensor.

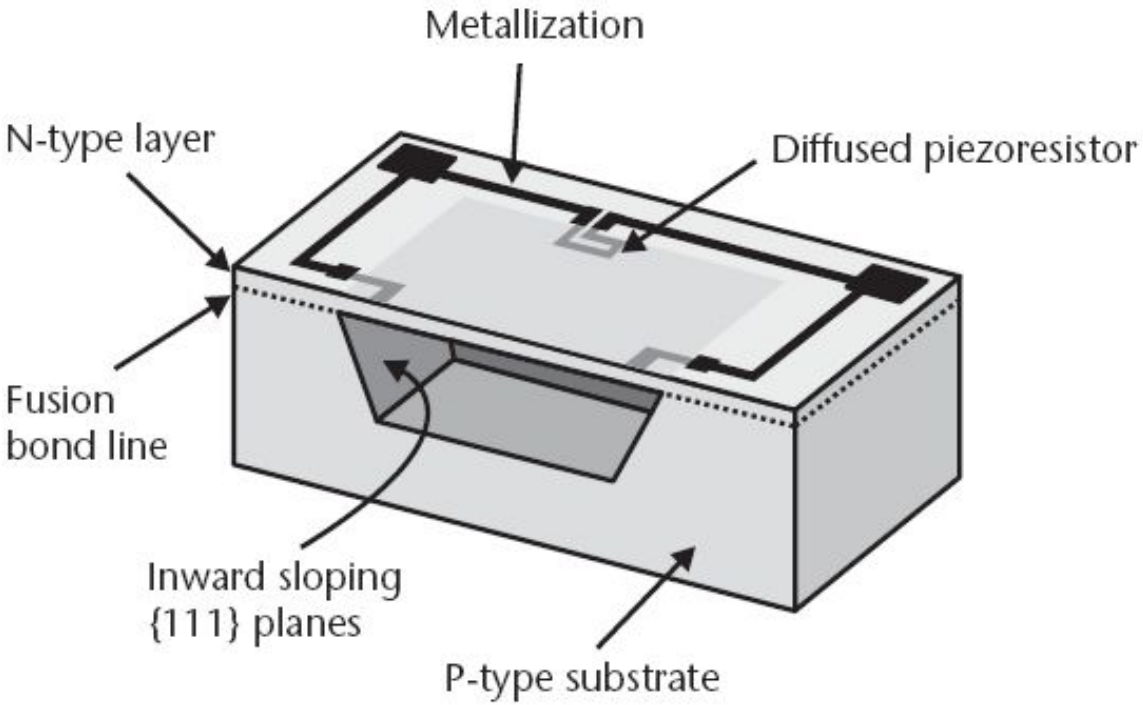

A miniature silicon-fusion-bonded absolute pressure sensor. (*Courtesy of:* GE NovaSensor of Fremont, California.) The sensor is 400 μm wide, 800 μm long, and 150 μm thick, and it fits inside the tip of a catheter.

Датчик давления Pressure sensor

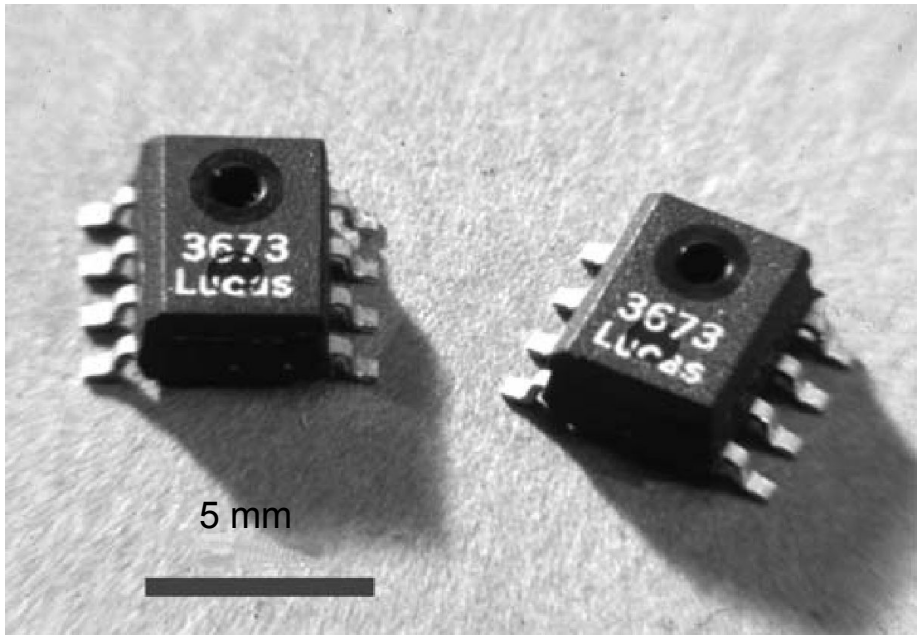

Photograph of the NovaSensor NPP-301, a premolded plastic, surface mount (SOIC-type) and absolute pressure sensor. (*Courtesy of:* GE NovaSensor of Fremont, California.)

Illustration of a premolded plastic package. Adapting it to pressure sensors involves incorporating fluid ports in the premolded plastic housing and the cap.

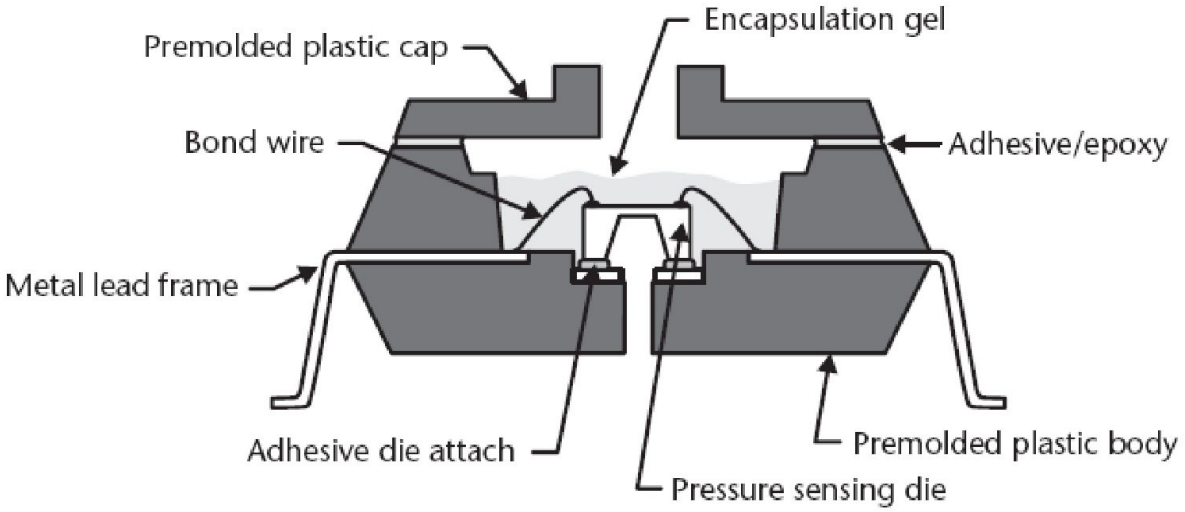

Датчик кровяного давления Blood pressure sensor

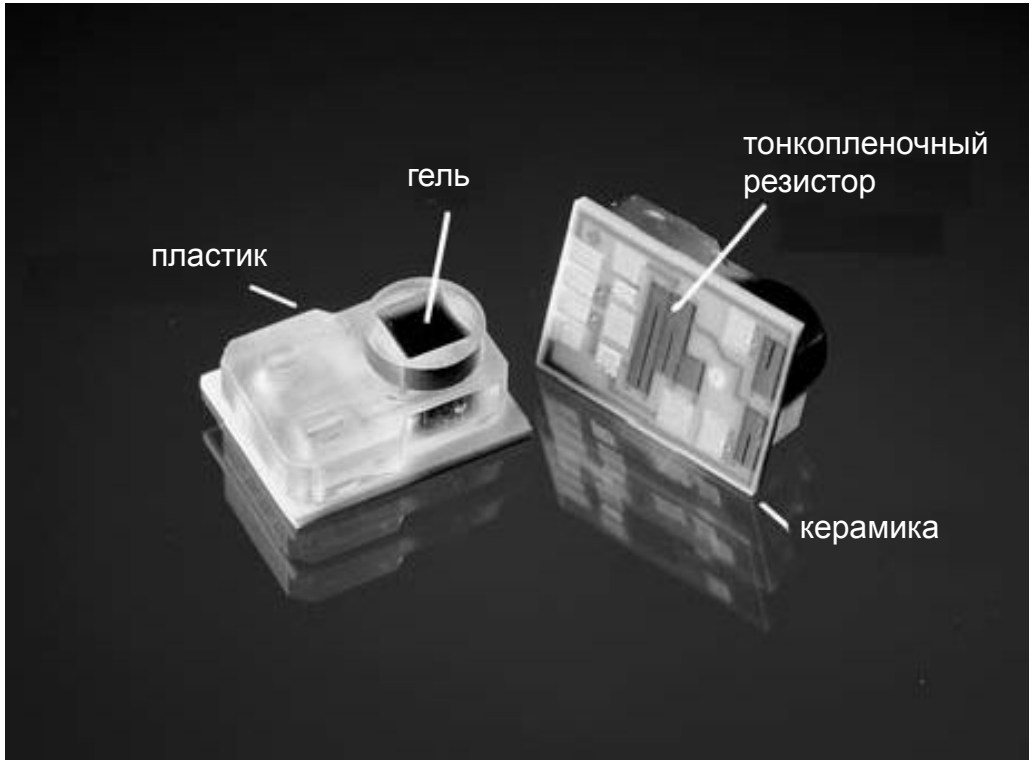

Photograph of a disposable blood pressure sensor for arterial-line measurement in intensive care units. The die (not visible) sits on a ceramic substrate and is covered with a plastic cap that includes an access opening for pressure. A special black gel dispensed inside the opening protects the silicon device while permitting the transmission of pressure. (*Courtesy of:* GE NovaSensor, Fremont, California .)

Высокотемпературный датчик давления
High-temperature pressure sensor

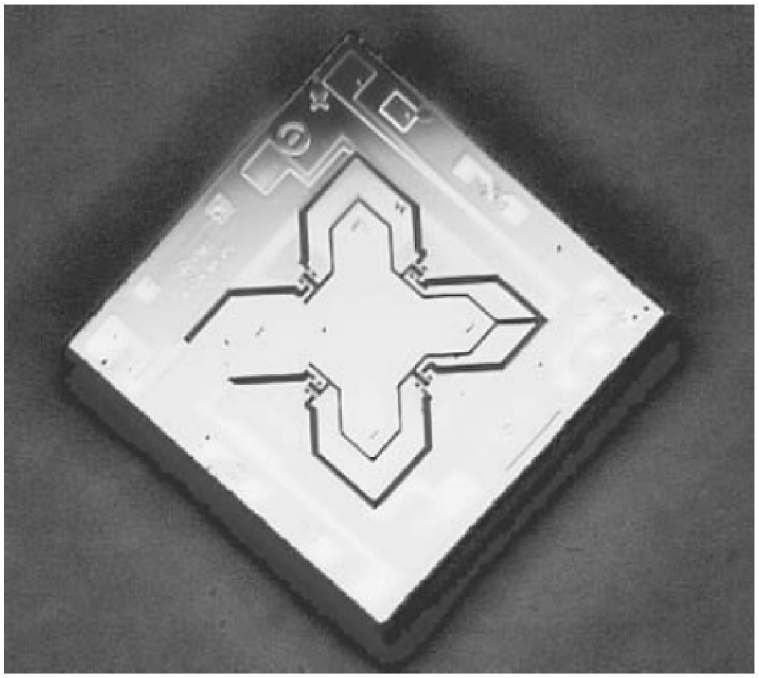

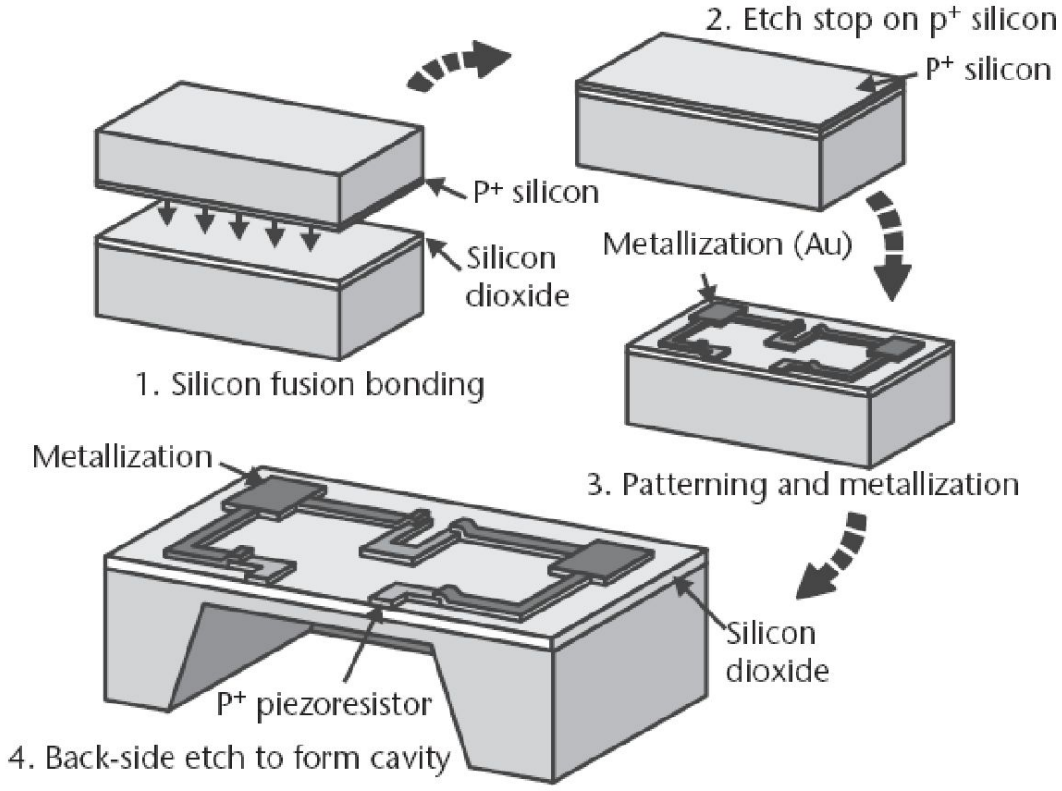

Photograph of an SOI-based pressure sensor rated for extended temperature operation up to 300°C (*Courtesy of:* GE NovaSensor of Fremont, California.) and its fabrication process.

Пьезоэлектрический элемент (датчик или привод)
Piezoelectric element (sensor or actuator)

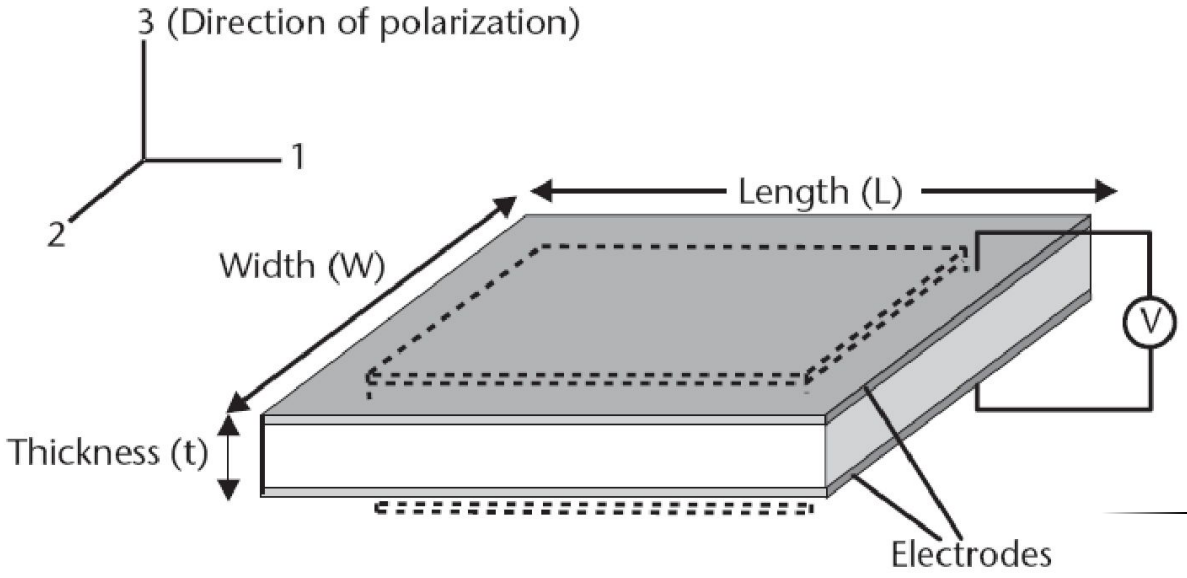

Active element

Активный элемент:

ZnO, $LiNbO_3$, $BaTiO_3$, $PbZrO_3$ or quartz

$$\Delta L = d_{31} \cdot V_a \cdot L/t$$

$$\Delta W = d_{31} \cdot V_a \cdot W/t$$

$$\Delta t = d_{33} \cdot V_a$$

An illustration of the piezoelectric effect on a crystalline plate. An applied voltage across the electrodes results in dimensional changes in all three axes (if d_{31} and d_{33} are nonzero). Conversely, an applied force in any of three directions gives rise to a measurable voltage across the electrodes.

$$V_m = d_{31} \cdot F/(\varepsilon \cdot W)$$

$$V_m = d_{31} \cdot F/(\varepsilon \cdot L)$$

$$V_m = d_{33} \cdot F \cdot t/(\varepsilon \cdot L \cdot W)$$

Пьезоэлектрические коэффициенты различных материалов Piezoelectric coefficients

Material	*Piezoelectric Constant (d_{ij}) (10^{-12} C/N)*	*Relative Permittivity (ε_r)*	*Density (g/cm^3)*	*Young's Modulus (GPa)*	*Acoustic Impedance (10^6 $kg/m^2 \cdot s$)*
Quartz	$d_{33} = 2.31$	4.5	2.65	107	15
Polyvinylidene-fluoride (PVDF)	$d_{31} = 23$ $d_{33} = -33$	12	1.78	3	2.7
$LiNbO_3$	$d_{31} = -4$, $d_{33} = 23$	28	4.6	245	34
BaTiO3	$d_{31} = 78$, $d_{33} = 190$	1,700	5.7		30
PZT ($PbZrO_3$)	$d_{31} = -171$ $d_{33} = 370$	1,700	7.7	53	30
zinc oxide (ZnO)	$d_{31} = 5.2$, $d_{33} = 246$	1,400	5.7	123	33

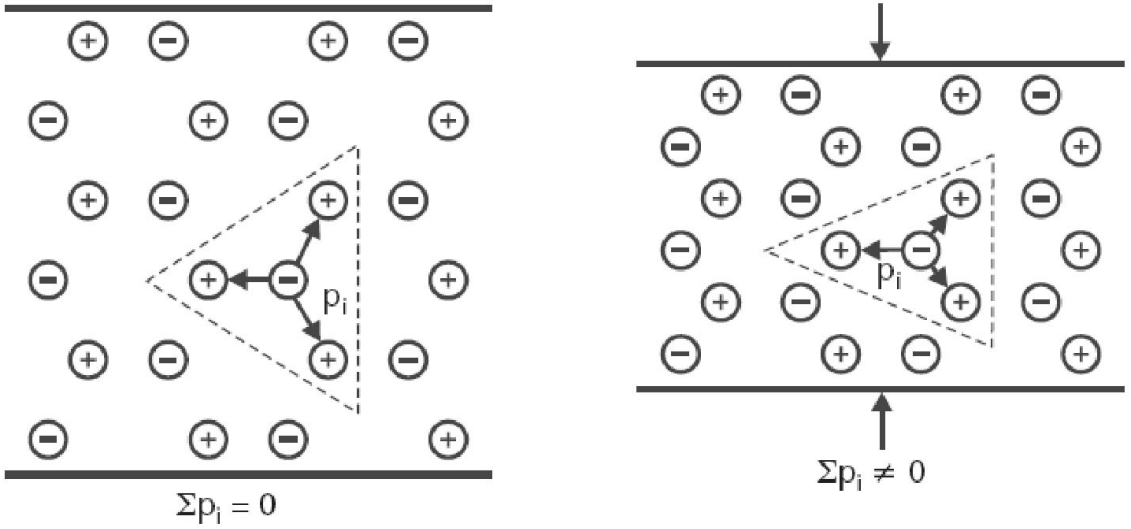

Датчики ускорения Acceleration sensor

Measurement	*Application*
Acceleration	Front and side airbag crash sensing
	Electrically controlled car suspension
	Safety belt pretensioning
	Vehicle and traction control systems
	Inertial measurement, object positioning, and navigation
	Human activity for pacemaker control
Vibration	Engine management
	Condition-based maintenance of engines and machinery
	Security devices
	Shock and impact monitoring
	Monitoring of seismic activity
Angles of inclination	Inclinometers and tilt sensing
	Vehicle stability and roll
	Headlight leveling
	Computer peripherals (e.g., joystick, head mounted displays)
	Handwriting recognition (e.g., SmartQuill from British Telecom plc)
	Bridges, ramps, and construction

Требования к датчикам ускорения
Requirements to acceleration sensors

- Accelerometers for airbag crash sensing are rated for a full range of ±50G and a bandwidth of about one kilohertz.
- Devices for measuring engine knock or vibration have a range of about 1G, but must resolve small accelerations (<100 μG) over a large bandwidth (>10 kHz).
- Modern cardiac pacemakers monitor the level of human activity, and correspondingly adjust the stimulation frequency. The ratings on such sensors are ±2G and a bandwidth of less than 50 Hz, but they require extremely low power consumption.
- Accelerometers for military applications can exceed a rating of 1,000G.
- Cross-axis rejection ratios in excess of 40 dB are always desirable.
- Shock immunity is defined in terms of a peculiar but more practical test involving dropping the device from a height of one meter over concrete - a dynamic peak of 10,000G with excitation of various resonant modes that may cause catastrophic failure.

The overall market for silicon microaccelerometers reached $319 million in 2000 and has continuously been growing. Cost of such devices has constantly been decreasing, for instance, from estimated $10 per unit in the early 1990s to less than $2 per unit in 2002.

Базовая структура датчика ускорения
Base structure of acceleration sensor

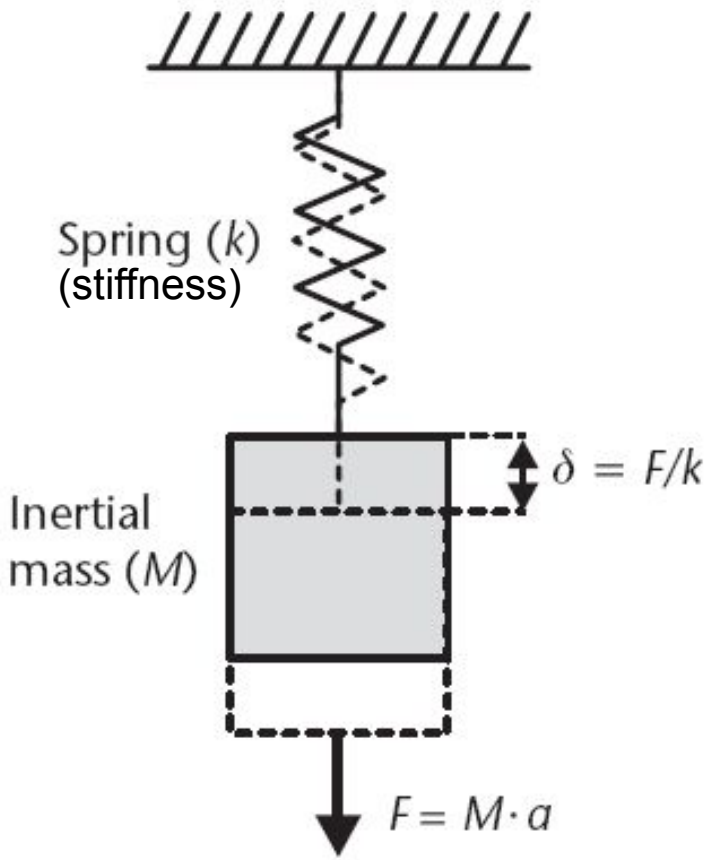

Resonant frequency:

$$f_r = \frac{1}{2\pi}\sqrt{\frac{k}{M}}$$

Noise equivalent acceleration:

$$a_{noise} = \sqrt{\frac{8\pi K_B T f_r B}{Q\,M}} \quad ; \quad B < f_r$$

K_B = Boltzmann constant

T = Temperature

B = Bandwidth

Q = Quality factor

The basic structure of an accelerometer, consisting of an inertial mass suspended from a spring. The resonant frequency and the noise-equivalent acceleration (due to Brownian noise) are given.

Пьезорезистивный датчик ускорения
Piezoresistive acceleration sensor

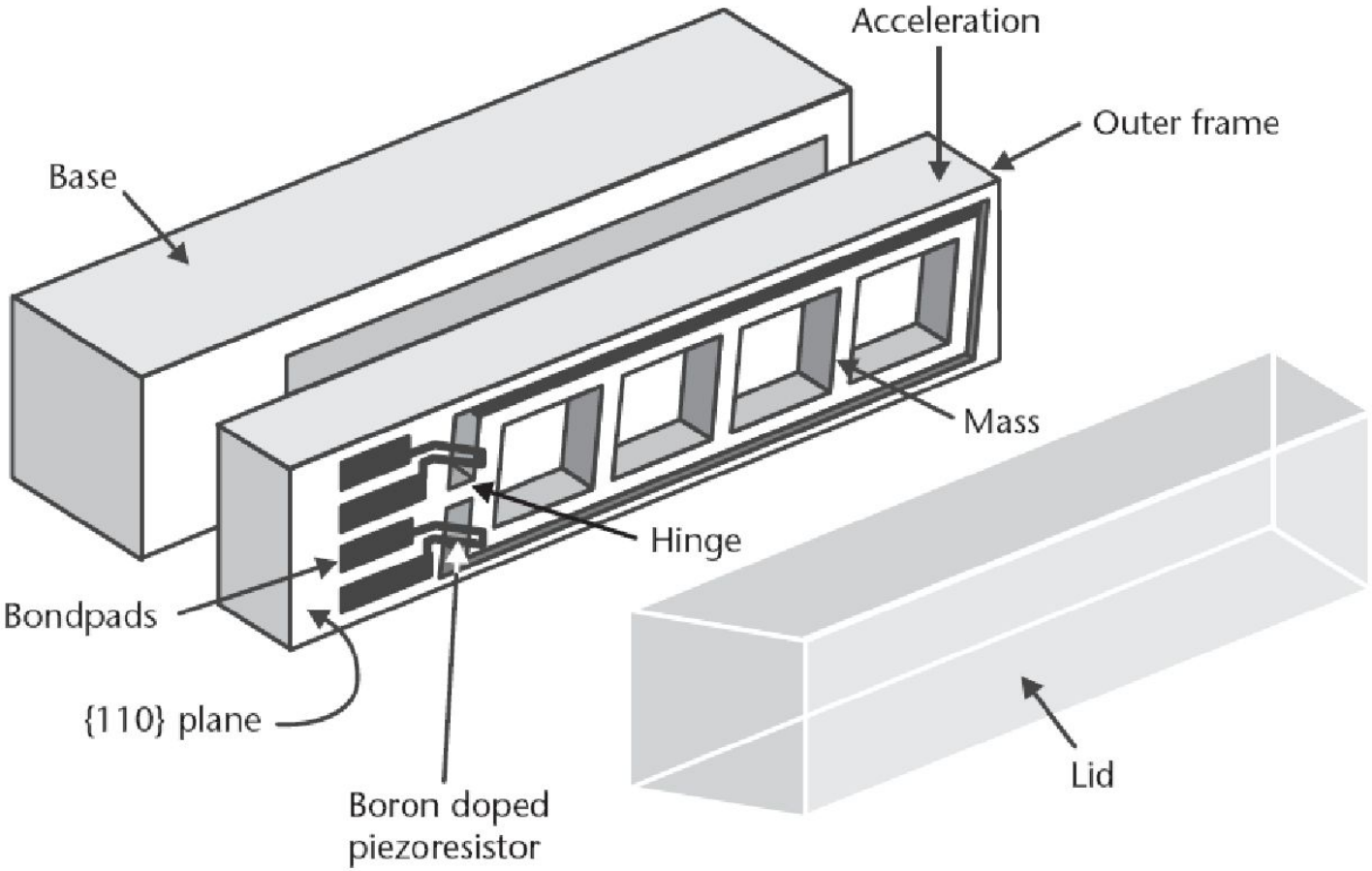

Illustration of a piezoresistive accelerometer from Endevco Corp., fabricated using anisotropic etching in a {110} wafer. The middle core contains the inertial mass suspended from a hinge. Two piezoresistive sense elements measure the deflection of the mass. The axis of sensitivity is in the plane of the middle core. The outer frame acts as a stop mechanism to prevent excessive accelerations from damaging the part. f_r=28 kHz. The piezoresistors are 0.6 μm thick and 4.2 μm long, aligned along <111> direction for maximum performance. The output in response to an acceleration of 1G is 25mV for a Wheatstone bridge excitation of 10V.

Емкостной датчик Capacitor sensor

Поперечная конфигурация

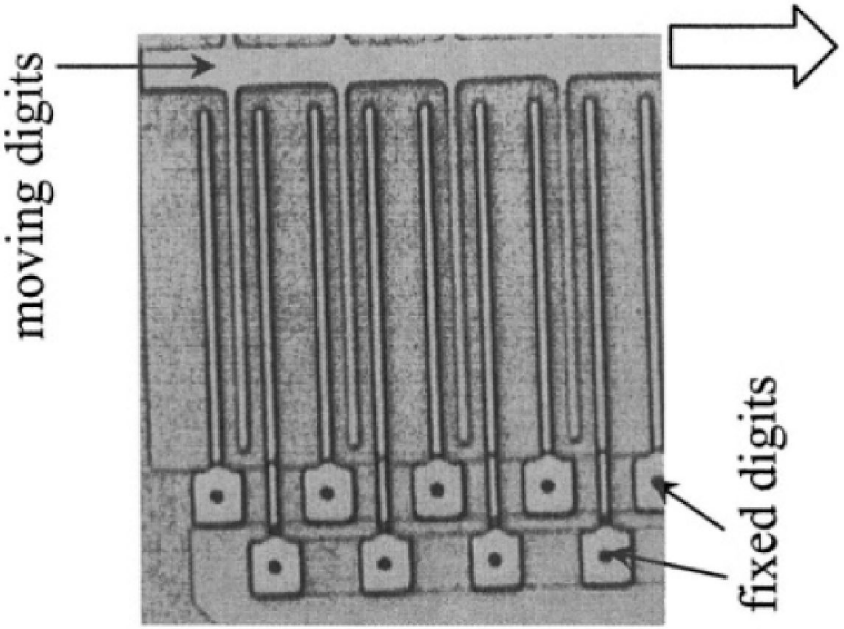

Продольная конфигурация

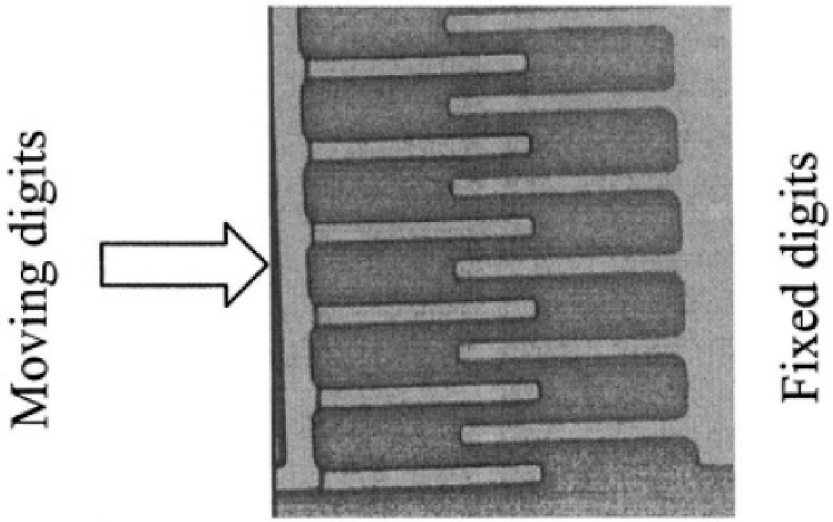

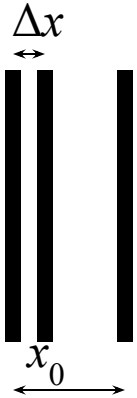

$$U = Q/C; \Delta U = -Q\Delta C/C^2 = -U\Delta C/C$$

$$\Delta C = \frac{\partial C}{\partial x}\Delta x$$

$$\frac{\partial C}{\partial x} = \frac{\varepsilon l_y l_z}{(x_0 - \Delta x)^2}$$

$$\Delta U = -Q\varepsilon l_y l_z / \Delta x$$

$$\Delta U = -U\Delta x/(x_0 - \Delta x)$$

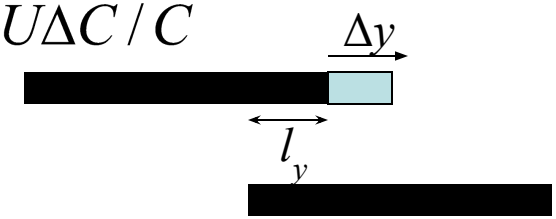

$$C = \varepsilon(l_y + \Delta y)l_z / x_0$$

$$\Delta C = \varepsilon \Delta y l_z / x_0$$

$$\Delta U = -U\Delta y/(l_y + \Delta y)$$

Емкостной датчик ускорения. Capacitive accelerometer.

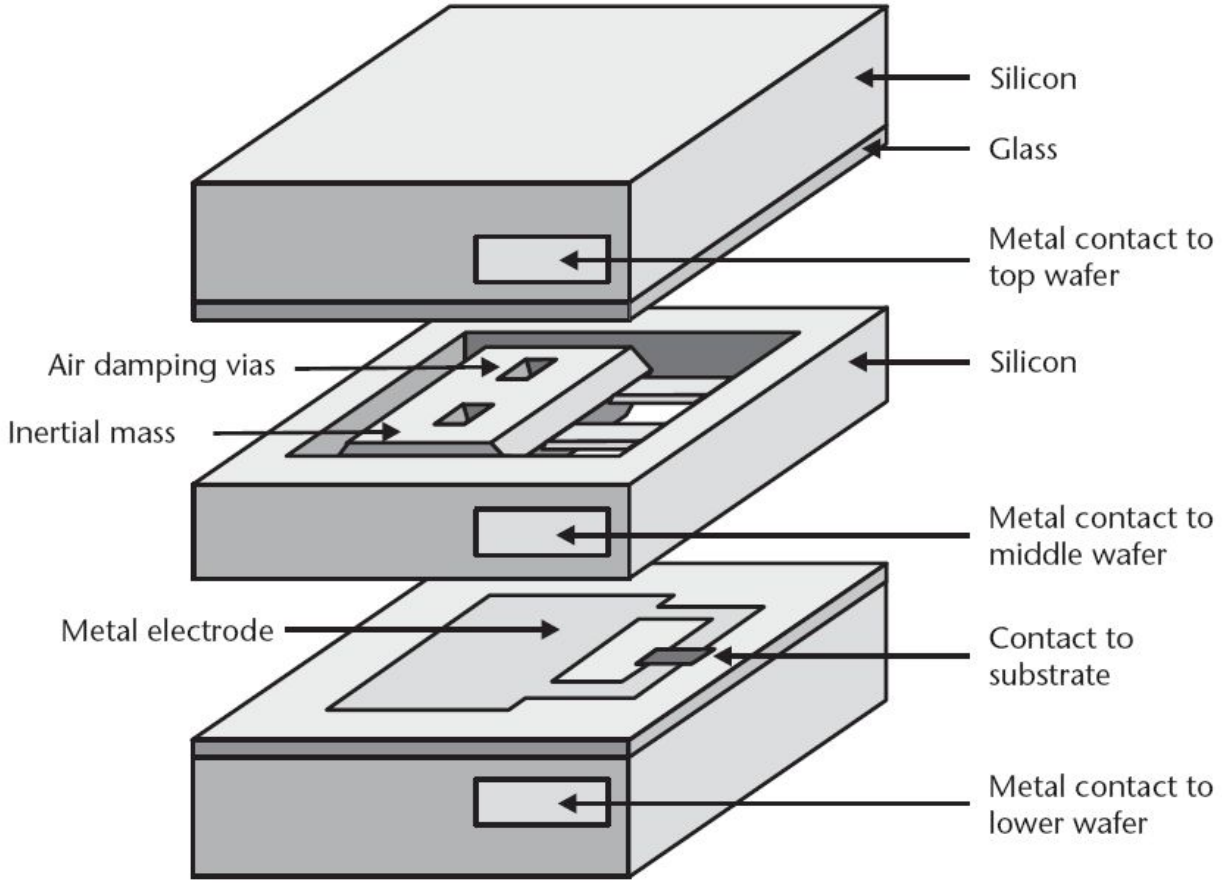

Illustration of a bulk micromachined capacitive accelerometer. The inertial mass in the middle wafer forms the moveable electrode of a variable differential capacitive circuit. Electronic circuits sense changes in capacitance, then convert them into an output voltage between 0 and 5V. The rated bandwidth is up to 400 Hz for the ±12G accelerometer, the cross-axis sensitivity is less than 5% of output, and the shock immunity is 20,000G. Measuring range is from ±0.5G to ±12G. (VTI Technologies of Vantaa, Finland.)

Емкостной датчик ускорения – последовательность производства
Production of capacitive accelerometer

1. Etch recess cavities in silicon

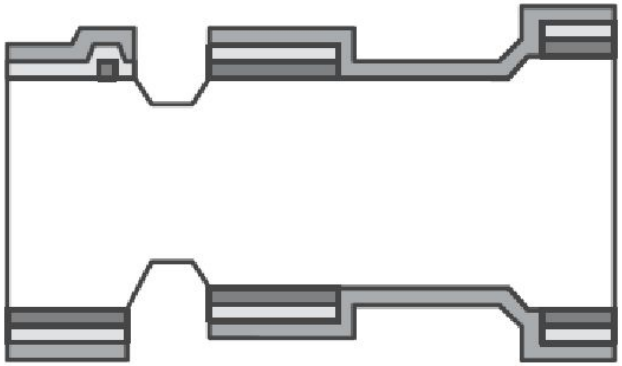

2. Deposit and pattern three masking layers; anisotropic etch silicon

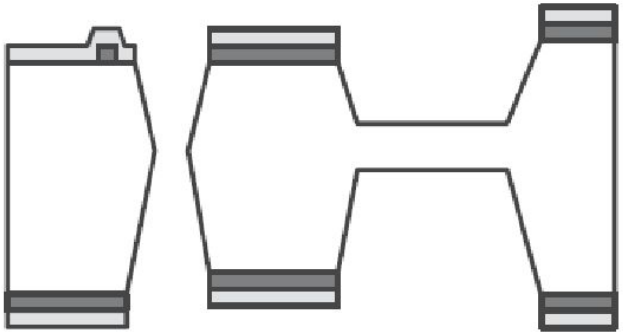

3. Remove first masking layer; anisotropic etch silicon

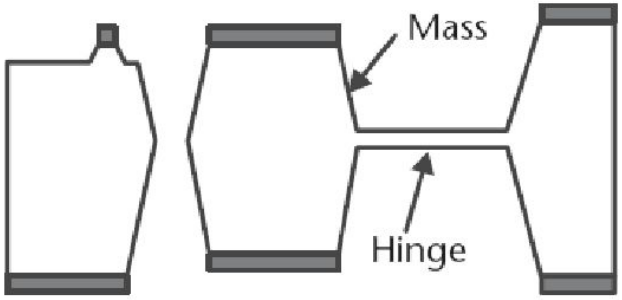

4. Remove second masking layer; anisotropic etch silicon

Емкостной датчик ускорения. Capacitive accelerometer.

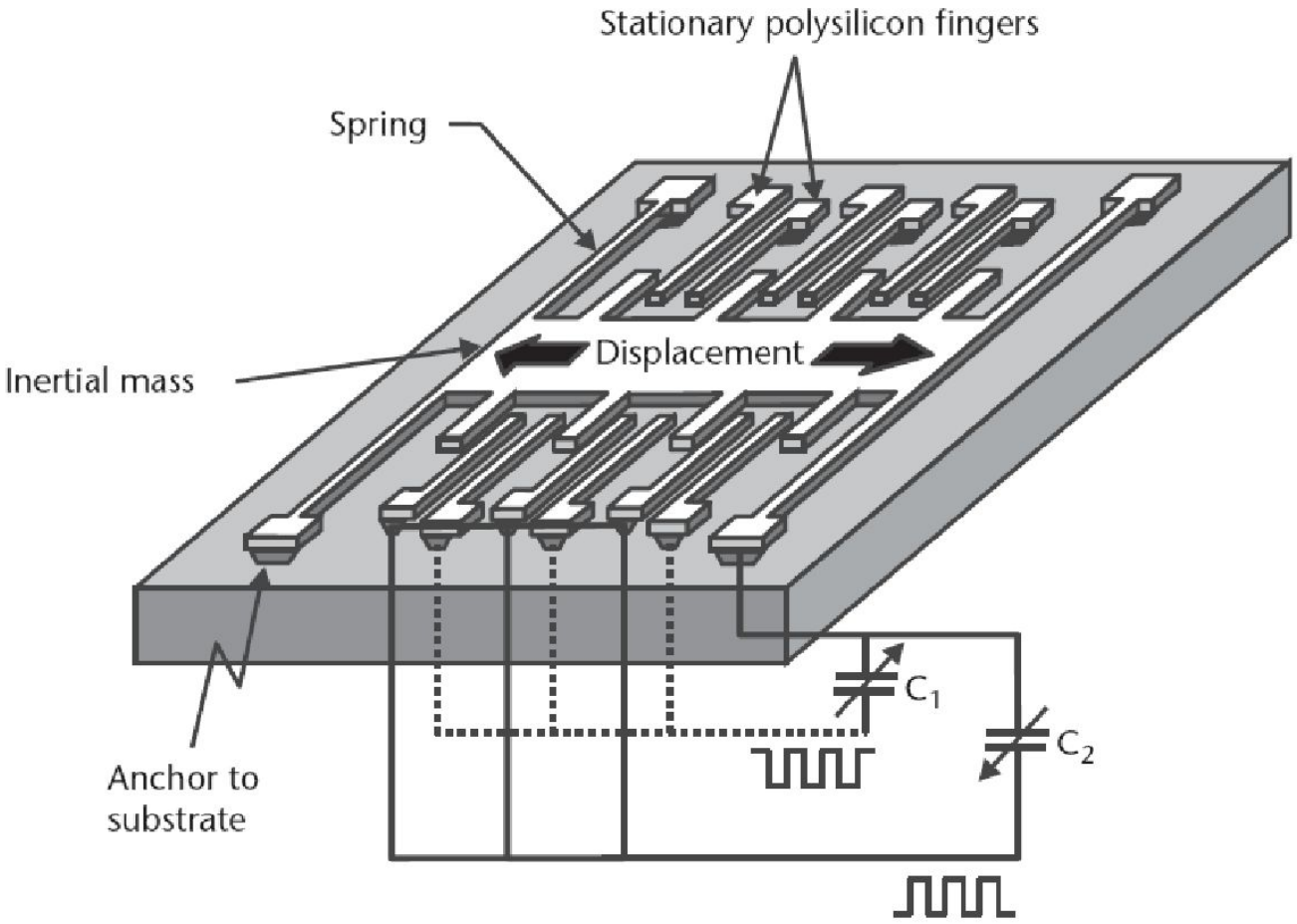

Acceleration rating is from 1G to 100 G, excitation frequency is 1 MHz, C = 10^{-13}F bandwidth is 1-6 kHz, mass is 0.3 - 100 μg, Brownian mechanical noise for 0.3 μg is 225 μ*G Hz*$^{1/2}$

Illustration of the basic structure of the ADXL family of surface micromachined accelerometers. A comb-like structure suspended from springs forms the inertial mass. Displacements of the mass are measured capacitively with respect to two sets of stationary finger-like electrodes. (Analog Devices, Inc., Norwood, Massachusetts, USA.)

Емкостной датчик ускорения, произведенный с помощью DRIE. Capacitive accelerometer using DRIE.

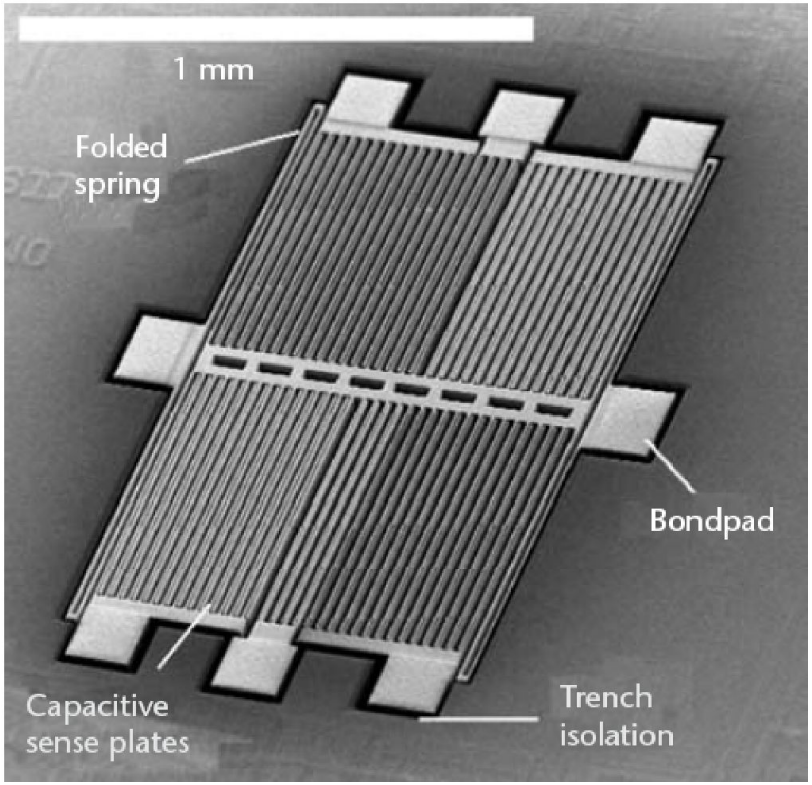

Scanning-electron micrograph of a DRIE accelerometer using 60-μm-thick comb structures. (Courtesy of: GE NovaSensor of Fremont, California.) Using structures 50 to 100 μm deep, the sensor gains an inertial mass, up to 100 μg, and a capacitance, up to 5 pF. The relatively large mass reduces mechanical Brownian noise and increases resolution. The high aspect ratio of the spring practically eliminates the sensitivity to *z*-axis accelerations.

Сравнение пьезорезистивного, емкостного и электромагнитного методов измерения
Comparison of different sensing

Piezoresistive	*Capacitive*	*Electromagnetic*
Simple fabrication	Simple mechanical structure	Structural complexity varies
Low cost	Low cost	Complex packaging
Voltage or current drive	Voltage drive	Current drive
Simple measurement circuits	Requires electronic circuits	Simple control circuits
Low-output impedance	Susceptible to EMI	Susceptible to EMI
High-temperature dependence	Low-temperature dependence	Low temperature dependence
Small sensitivity	Large dynamic range	Sensitivity $\propto$ magnetic field
Insensitive to parasitic resistance	Sensitive to parasitic capacitance	Insensitive to parasitic inductance
Open loop	Open or closed loop	Open or closed loop
Medium power consumption	Low power consumption	Medium power consumption

To be continued

Домашнее задание

...